https://doi.org/10.5194/egusphere-2023-941
Preprint. Discussion started: 11 May 2023
© Author(s) 2023. CC BY 4.0 License.

The global correlation between internal-tide generation and the depth-distribution of cold-water corals

Anna-Selma van der Kaaden[1,2], Dick van Oevelen[1], Christian Mohn[3], Karline Soetaert[1], Max Rietkerk[2], Johan van de Koppel[1], Theo Gerkema[1]

[1] NIOZ Royal Netherlands Institute for Sea Research, Department of Estuarine and Delta Systems, PO Box 140, 4400 AC Yerseke, The Netherlands
[2] Copernicus Institute for Sustainable Development, Department of Environmental Sciences, Utrecht University, The Netherlands
[3] Department of Ecoscience, Aarhus University, Roskilde, Denmark

Correspondence to: Anna van der Kaaden (annavanderkaaden@gmail.com)

Abstract. Internal tides are known to be an important source of mixing in the oceans, especially in the bottom boundary layer. The depth of internal-tide generation therefore seems important for benthic life and the formation of cold-water coral mounds, but internal-tidal conversion is generally investigated in a depth-integrated sense. Using both idealized and realistic simulations on continental slopes, we found that the depth of internal-tide generation increases with increasing slope steepness and decreases with intensified shallow stratification. The depth of internal-tide generation also shows a typical latitudinal dependency. Using a global database of cold-water corals, we found that the depth-pattern of internal-tide generation is remarkably similar to the depth-pattern of cold-water corals globally: shallowest near the poles and deepest around the equator with a shoaling around 25 degrees South and North and shallower north of the equator than south of the equator.

We further found that cold-water corals are, more than what would be expected by chance, associated to the (super)critical reflection of internal tides (i.e., situated on topography that is steeper than the internal tidal beam) and to trapped internal tides (i.e., above the critical latitude of 70 degrees for semidiurnal tides and 30 degrees for diurnal tides). The (super)critical reflection of internal tides and trapped internal tides therefore provide an interesting new angle of food supply mechanisms that has not yet been considered in cold-water coral studies. With climate change, stratification is expected to increase. Based on our results, this would cause a shoaling of internal-tide generation, possibly creating new shallower suitable habitat for cold-water corals on continental slopes.

1. Introduction

The tide-generating force exerted by the sun and moon on the oceans causes long waves to travel over the ocean surface, called the barotropic tides. In the simplest case of a non-stratified ocean with flat topography, the water parcels move horizontally in unison across the water column, along with a rise and fall of the ocean surface, typically at a diurnal or semidiurnal frequency. In reality, the ocean is stratified (layered) and has complex topography, giving rise to waves that travel in the interior of the ocean, as a movement of the isopycnals (levels of constant density). These baroclinic or 'internal' tides are an important

https://doi.org/10.5194/egusphere-2023-941
Preprint. Discussion started: 11 May 2023
© Author(s) 2023. CC BY 4.0 License.

mechanism for mixing in the ocean (Vic et al., 2019; st. Laurent and Garrett, 2002; Garrett and Kunze, 2006). With amplitudes of hundreds of meters and associated turbulent cascades, internal tidal waves contribute to the redistribution of organic matter, nutrients, heat, and salinity between the deeper and shallower ocean (Sarkar and Scotti, 2017; Jackson et al., 2012).

The internal tide thus increases the exchange of nutrients and organic matter between the deep- and shallower ocean, and by extension also increases benthic-pelagic coupling (Turnewitsch et al., 2016). Benthic organisms, such as cold-water corals, rely on organic matter that ultimately originates from primary production at the sea-surface (van Oevelen et al., 2018; van Engeland et al., 2019; Carlier et al., 2009). During its journey towards the deep-sea, organic matter is degraded by organisms in the water column, decreasing the food quantity and quality for benthic life with water depth (Snelgrove et al., 2017; Nakatsuka et al., 1997). Internal tidal dynamics can accelerate the vertical transport of organic matter towards the seafloor and stimulate benthic life by increasing food availability (Soetaert et al., 2016; Vic et al., 2019; st. Laurent and Garrett, 2002).

Cold-water coral reefs are deep-sea ecosystems that have a particularly high organic-matter processing rate and have indeed been associated with internal (tidal) waves (e.g., Davies et al., 2009; Hanz et al., 2019; Juva et al., 2020; Mohn et al., 2014; Roberts et al., 2021; van Haren et al., 2014; Wang et al., 2019). Cold-water coral reefs and mounds are built up of dead coral framework and coral rubble, often with thriving cold-water coral reefs on the mound tops. Using 6-hourly output from a 3D hydrostatic model, van der Kaaden et al. (2021) calculated the energy conversion rate (EC) from barotropic to baroclinic tides over a smoothed bathymetry of the Rockall Bank margin and found that the region of highest EC corresponds to the present-day location of cold-water coral mounds. This suggests that the internal tide also plays a role in determining the region of coral mound initiation.

The depth-integrated and global total energy contained in the internal tide has been investigated (e.g., St. Laurent & Garrett, 2002; Vic et al., 2019), but the depth of internal-tide generation has not yet been considered in the present context and on a global scale. Yet, the depth of internal-tide generation is likely of relevance to cold-water corals, since it is at the depth where internal tides are generated that the highest internal wave excursions occur near the seafloor (Mohn et al., 2014; van der Kaaden et al., 2021; Frederiksen et al., 1992).

Internal tides can be generated on continental slopes. The wave energy in these internal tides propagates away from the topography diagonally. So, internal tidal waves travel away from the topography as a beam that makes an angle to the horizontal (Fig. 1). The steepness (i.e., the tangent of the angle with the horizontal) of the continental slope (s) compared to the steepness of the beam (a) is a key factor determining the strength of internal-tide generation. The bottom slope is critical when slope steepness equals the beam steepness ($s = a$); gentler bottom slopes are subcritical ($s < a$) and steeper slopes are supercritical ($s > a$). Since the wave angle of the M2 tide is rather gentle (3-8 degrees or a steepness of 0.05-0.14, i.e., 5-14 %) most continental slopes have a region of near critical steepness for the M2 tide (Sarkar and Scotti, 2017), where intensification of beams occurs.

The beam steepness (a) is given by Eq. (1):

$$a = \sqrt{\frac{\omega^2 - f^2}{N^2 - \omega^2}} \quad (1)$$

https://doi.org/10.5194/egusphere-2023-941
Preprint. Discussion started: 11 May 2023
© Author(s) 2023. CC BY 4.0 License.

with ω the tidal wave frequency in rad/s, i.e., $1.4052 \cdot 10^{-4}$ rad/s for the semidiurnal M2 tidal constituent and $0.7292 \cdot 10^{-4}$ rad/s for the diurnal K1 tidal constituent. The beam steepness depends on the Coriolis frequency (f) and on how strongly gravity acts as a restoring force, i.e., the buoyancy frequency (N). The former is related to latitude: zero at the equator and increasing towards the poles. The latter is related to stratification: a steeper density gradient results in larger values for N. The depth and magnitude of the internal tide can thus be expected to vary with 1) continental slope steepness, 2) latitude, and 3) stratification. At latitudes where the Coriolis frequency exceeds the frequency of the tidal constituent, the wave energy in the internal tide cannot propagate away from the topography. The internal tide is then said to be 'trapped' at the topography. Similarly as with 'critical slopes', near these 'critical latitudes' (around 70 degrees for the M2 tide and around 30 degrees for the K1 tide), strong currents and enhanced vertical mixing occur at the region of internal-tide generation (Pereira et al., 2002).

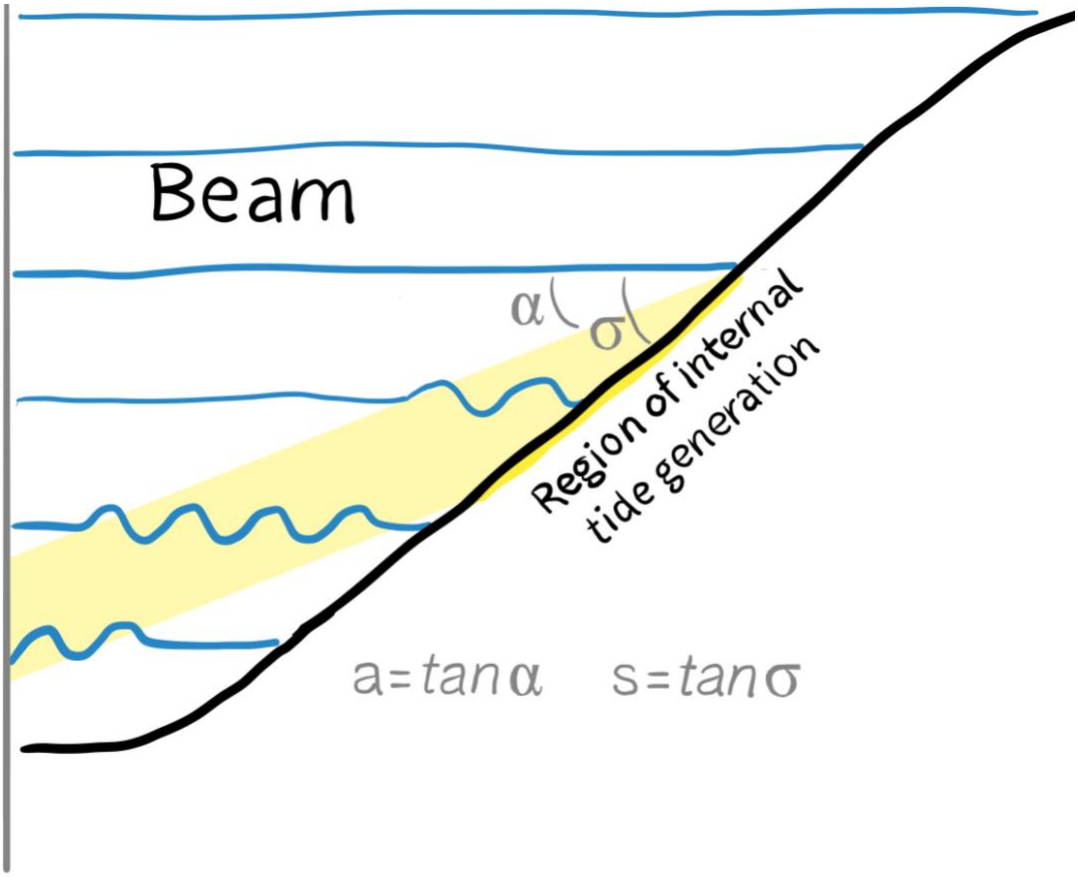

Figure 1. Sketch of internal-tide generation on a continental slope. Internal tidal waves travel on the surface of isopycnals (blue lines). The energy in the internal tide (i.e., amplitude) travels away from the topography in the horizontal as well as in the vertical, forming a beam (yellow). The angle of the beam to the horizontal (α) as compared to the angle of the continental slope (σ) is a parameter determining the depth and strength of internal-tide generation on the seafloor.

Here, we investigated how the depth of the internal tide on the continental slope changes along realistic transects extracted at different latitudes and continental slopes. The energy conversion rate of barotropic to baroclinic tides is taken as a proxy for

https://doi.org/10.5194/egusphere-2023-941
Preprint. Discussion started: 11 May 2023
© Author(s) 2023. CC BY 4.0 License.

the strength of internal tides. We investigated the relationship between the depth of internal-tide generation on the continental slope and slope steepness, latitude, and stratification, with an idealized model setup and with realistic topography and buoyancy frequencies from transects. To study the importance of tidal dynamics for cold-water coral reefs, we then compared the depth of internal-tide generation on the continental margin to occurrences of reef-building cold-water corals. This study contributes to the general understanding of the role of the internal tide for cold-water coral communities.

2. Methods

2.1 Model description

Energy conversion from the barotropic to baroclinic tide (EC) was simulated with a linear hydrostatic internal-tide generation model. We assume uniformity in topography and all dynamic variables in the along-slope direction (y), making the model essentially 2D (except for a transverse velocity component v that is induced by the Coriolis force). This approach can be justified since continental slopes vary mostly in the across-slope direction. A stream function can thus be introduced for the baroclinic cross-slope and vertical current speeds: $u = {}^{\partial\psi}/_{\partial z}$ and $w = -{}^{\partial\psi}/_{\partial x}$ respectively, resulting in the following linear hydrostatic model equations (Gerkema et al., 2004):

$$\frac{\partial^3\psi}{\partial z^2\partial t} - f\frac{\partial v}{\partial z} + \frac{\partial b}{\partial x} = 0, \quad (2)$$

$$\frac{\partial v}{\partial t} + f\frac{\partial \psi}{\partial z} = 0, \quad (3)$$

$$\frac{\partial b}{\partial t} - N^2\frac{\partial \psi}{\partial x} = -\frac{zN^2 Q\sin\omega t}{[H-h(x)]^2}\frac{dh}{dx} \quad (4)$$

where f is the Coriolis parameter and b the buoyancy frequency expressed as "minus effective gravity" $b = g\frac{\rho}{\rho^*}$ (m s^{-2}) with ρ^* a constant representative value of density (kg m^{-3}) and ρ the density perturbation with respect to the local static value. The right-hand side of Eq. (4) represents the forcing of the cross-slope barotropic tidal flux with amplitude Q and semidiurnal (M2) tidal frequency σ ($1.4052\cdot10^{-4}$ rad s^{-1}).

The bottom is described by $z = -H + h(x)$, where H is the undisturbed ocean depth, $h(x)$ the topography, and a rigid lid surface is located at $z = 0$. The model was solved with a Chebychev collocation method using 60 Chebychev polynomials. In the vertical, we used 60 topography-following vertical model layers with increased vertical resolution near the surface and bottom. In the horizontal direction and in time, a finite-difference method was used with steps of 0.4 km, and a temporal resolution of 1,000 time-steps per tidal period. A sponge layer of 150 km in the deep ocean and 50 km on the shelf dampened incoming waves with a Rayleigh-friction term and a fourth-order spatial filter was applied to dampen fine-scale artificial oscillations. The model was forced with a barotropic cross-slope flux of 100 m^2 s^{-1} for all simulations. For further details on the numerical scheme, we refer to Gerkema et al. (2004).

https://doi.org/10.5194/egusphere-2023-941
Preprint. Discussion started: 11 May 2023
© Author(s) 2023. CC BY 4.0 License.

The amount of energy that is converted from the barotropic into the baroclinic tide per second, per volume (W m^{-3}) is calculated as:

$$EC = -\frac{\rho^*}{T}\int_0^T dt\, b\, W \quad (5)$$

with T one tidal period and W the barotropic vertical velocity (m s^{-1}).

For the simulations, we focussed on the M2 tide, since the semidiurnal (or mixed semidiurnal) tide is dominant at most places regarding both surface elevations (Gerkema, 2019) and barotropic tidal current speed (Fig. 2 constructed using data from the TPXO9 atlas).

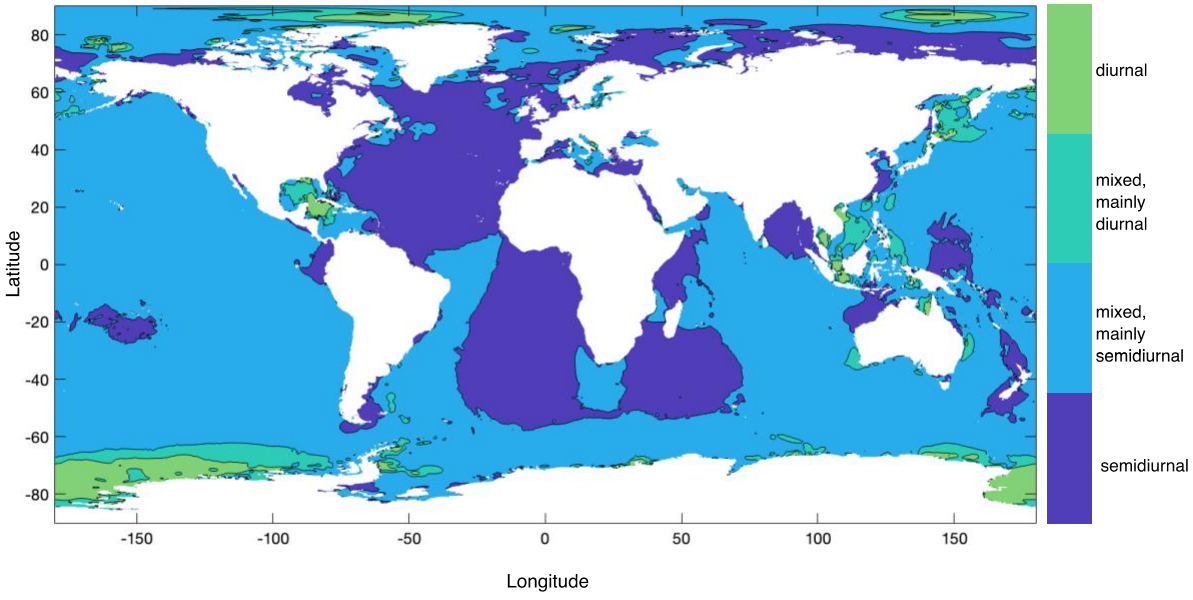

Figure 2. Global distribution of semidiurnal (dark blue), diurnal (green) and mixed tides. The classification is based on barotropic tidal current amplitudes of the semidiurnal M2 and S2 tide and the diurnal K1 and O1 tide, as derived from the TPXO9 atlas. The classification is based on the so-called form factor, as in Gerkema (2019), and was calculated as the sum of amplitudes of the K1 and O1 constituents over the sum of those of M2 and S2 constituents. This map was created with the TPXO9 atlas (Egbert and Erofeeva, 2002).

2.2 Data

2.2.1 Bathymetry, stratification, and surface tides

Bathymetry for the global transects was extracted from the NOAA ETOPO1 global relief model (NOAA National Geophysical Data Center, 2009, accessed June 2022) with the *marmap* package in R (Pante and Simon-Bouhet, 2013). The topography has a spatial resolution of 1 arcminute, equivalent to a mean resolution of 1.89 km (0.71 km - 24.63 km, min - max).

Realistic stratification profiles were selected per season by calculating buoyancy frequency values (N) using salinity and temperature data from the Levitus seasonal dataset (Levitus, 1982). The Levitus database includes salinity and temperature in the ocean at 24 levels ranging from the surface down to 1500 m and was last updated May 2015. The seasonal dataset includes

https://doi.org/10.5194/egusphere-2023-941
Preprint. Discussion started: 11 May 2023
© Author(s) 2023. CC BY 4.0 License.

4 seasons that are specified as: 1) February to April ('spring'), 2) May to July ('summer'), 3) August to October ('autumn'), 4) November to January ('winter'). Note that we classified the seasons with respect to the Norther Hemisphere, so e.g., February to April is NH spring but Southern Hemisphere autumn.

Information on surface tides came from the global barotropic tidal model TPXO9-atlas v5 (Egbert and Erofeeva, 2002). Barotropic horizontal tidal current speeds are provided at 1/30 degree resolution.

2.2.2 Database of cold-water coral occurrences

A global dataset of the occurrences of cold-water corals originated from the NOAA National Database for Deep-sea Corals and Sponges (NOAA National Database for Deep-Sea Corals and Sponges, version 20220426-0), ICES Vulnerable Marine Ecosystems (International Council for the Exploration of the Sea, June 2022) and OBIS (OBIS, 2022). From the NOAA database we selected all records of the main cold-water coral reef-building species *Desmophyllum pertusum* (previously *Lophelia pertusa*), *Enallopsammia profunda*, *E. pusilla*, *E. rostrata*, *Goniocorella dumosa*, *Madrepora carolina*, *M. oculata*, and *Solenosmilia variabilis* (Freiwald et al., 2004), below 100 m depth, recorded from 1900 or later, with a horizontal location accuracy of 1,000 m or less, and between the critical latitudes for the M2 tide of 70 degrees North and South (15,629 records). From ICES VME, we selected all "Stony corals" VME indicators in VME habitat type "Cold-water coral reef" with a position accuracy of 1,000 m or less, and between 70 degrees North and South (379 records). From OBIS, we selected all records of the main reef-building species (see above), below 100 m depth, with a location accuracy of 1,000 m or less, and between 70 degrees North and South (26,117 records). These records are excluding all records where the stated depth was incongruous with the topographic dataset (i.e., exceeding the depth of the bathymetry or with a location on land), or with nonsensical latitude and longitude coordinates. We also excluded all coral records marked as "dead" or "fossil". Our database contains 40,902 records in total. We used the ("middle") latitude and longitude coordinates and the mean depth.

We calculated the local slope steepness at which cold-water corals are found from ETOPO bathymetry at a 30 arc-minute resolution in R, in the same way as we calculated the slope of the smoothed model topography (next section 2.3.2). In the comparison between simulations, we only included those coral occurrences that are situated in regions where the barotropic tide is semidiurnal or mixed but mainly semidiurnal (as in Fig. 2).

2.3 Simulation settings

2.3.1 Idealized simulation setting

The relationship between internal-tide generation and topographic slope was investigated by running the model with various maximum topographic slopes, using the following values: 0.0228, 0.0285, 0.038, 0.057, 0.076, 0.114, 0.1425, 0.1899, 0.2279, and 0.2848. The relationship between internal-tide generation and latitude was investigated by running the model at latitudes of -70, -60, -50, etc. up to 70 degrees. The relationship between internal-tide generation and stratification was investigated with a vertically non-uniform stratification (N). We interpolated N from 0.001 rad s^{-1} at the ocean surface to a value at 100 m

https://doi.org/10.5194/egusphere-2023-941
Preprint. Discussion started: 11 May 2023
© Author(s) 2023. CC BY 4.0 License.

depth that represents a thermocline. At 100 m depth, we varied N from 0.001 rad s^{-1} to 0.005 rad s^{-1}, at steps of 0.0005 rad s^{-1}. We interpolated N from the value at 100 m depth to 0.001 rad s^{-1} at 3 km depth. The N -profile was smoothened before model simulation by cubic interpolation. All simulations were run for 20 tidal periods (starting from rest), after which the signal had become periodic over the slope.

2.3.2 Realistic simulation setting

For the realistic simulation setting, we selected transects perpendicular to all continental slopes at every 10th latitudinal degree between 64.5 degrees South and 64.5 degrees North. Selection was done by hand, resulting in 116 transects. Since the model by Gerkema et al. (2004) assumes that a continental shelf is present, only transects starting from a well-defined continental shelf were included in the analysis. Transects where the tidal signal was not periodic at the end of the simulations were excluded from the analysis, since the results on internal tide conversion rate would not be reliable in these cases. We thereby excluded 32 transects, resulting in 84 of the 116 transects being used in the analyses (Fig. 3).

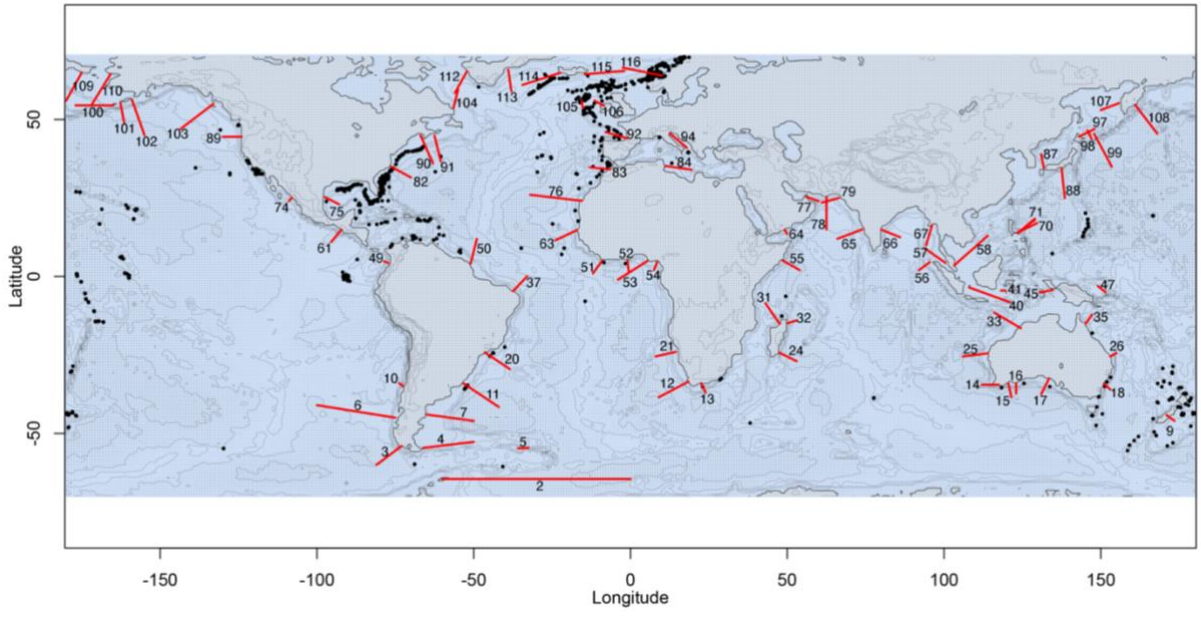

Figure 3. Map of the 84 (out of 116) selected transects (red lines) on which internal-tide generation was simulated with realistic topography and stratification. Some transects overlap with coral occurrences from the database (black dots). This map was created using the NOAA ETOPO1 global relief model (NOAA National Geophysical Data Center, 2009).

We investigate the depth of internal-tide generation on continental slopes. To avoid interference and scattering by internal-tide generation on rough topography (e.g., abyssal hills and canyons), we smoothed the bathymetry by placing the mean value of every 30 points (30 arcminutes) in the middle of those 30 points. The smoothed model topography was then built by making a cubic interpolation between the remaining averaged points at 0.4 km resolution. Realistic stratification profiles used in the model were assumed horizontally uniform along the cross-slope transects. For the model setup we selected the stratification profile located at the deepest part of the transect and extrapolated N from 5 m depth to the sea surface. For transects deeper

https://doi.org/10.5194/egusphere-2023-941
Preprint. Discussion started: 11 May 2023
© Author(s) 2023. CC BY 4.0 License.

than 1450 m depth, we set the value of N at the maximum transect depth to $2 \cdot 10^{-4}$ rad s^{-1}. Our approach can be justified, because stratification typically changes very little below 1.5 km depth and is not well-mapped (Banyte et al., 2018). Also, while stratification at the boundaries of deep water masses can cause internal wave generation, this happens typically on rough topography in the open ocean (Nikurashin and Ferrari, 2013; Banyte et al., 2018) whereas we focus on continental slopes. The buoyancy frequency along the vertical layers of the internal tide model was derived by cubic interpolation.

We identified peaks in energy conversion rates (EC) at the model seafloor in all transects with Matlabs *findpeaks* function. Since we forced all transect simulations with the same barotropic flux, EC rates are not realistically comparable between transects. We thus first scaled EC rates on transects between 0 and 1 and identified all peaks with a minimum prominence of 0.05. We further calculated the effective depth ($\bar{z}$) of internal-tide generation weighted by EC rates as Eq. (6):

$$\bar{z} = \frac{1}{max(z) - \min(z)} \cdot \frac{\int_{min(z)}^{max(z)} z \cdot EC(z) dz}{\int_{min(z)}^{max(z)} EC(z) dz} \quad (6)$$

This way, the effective depth of generation really indicates where the bulk of the generation takes place (rather than being controlled by incidental narrow peaks in EC). Similarly, we calculated the weighted mean slope steepness and weighted mean latitude. We ignored negative EC values, since negative values indicate a loss of energy from the baroclinic tide instead of a generation. See Fig. A1 (appendix A) for an example transect with EC peaks and weighted mean depth.

3. Results

We investigated the relationship between the depth of internal-tide generation and slope steepness, latitude, and stratification with simulations in an idealized setting and globally in a realistic setting. For this, we use the energy conversion rate (EC) from the barotropic to the baroclinic tide at the model seafloor as a proxy for the generation of internal tides and associated mixing. We then compared the depth of internal-tide generation to the depth at which cold-water corals occur from a global database of cold-water coral occurrences.

3.1 Idealized simulations

With increasing mean slope steepness, EC rates at the seafloor intensify (Fig. 4a). For slopes with a steepness <0.03, the depth of maximum EC decreases with increasing slope steepness and for slopes with a steepness >0.06, the depth of maximum EC increases with increasing slope steepness from about 1 km to 0.3 km depth. The depth of maximum EC increases from about 0.25 km depth near the poles to about 0.6 km depth at the equator (Fig. 4b). EC rates intensify towards the equator, regardless of stratification and intensify with increasing stratification (Fig. 4c). The depth of maximum EC decreases with increasing stratification from about 0.9 km depth at a stratification of $1.5 \cdot 10^{-3}$ rad s^{-1} to 0.3 km depth at a stratification of $5 \cdot 10^{-3}$ rad s^{-1}.

https://doi.org/10.5194/egusphere-2023-941
Preprint. Discussion started: 11 May 2023
© Author(s) 2023. CC BY 4.0 License.

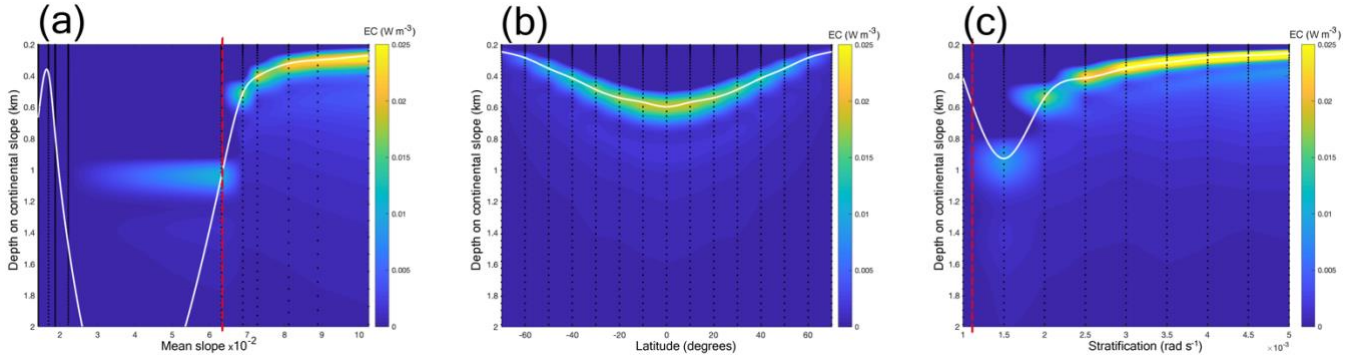

Figure 4. Panels depict energy conversion (EC) on the continental slope (colours) for different mean slope steepness (a), latitude (b), and stratification (*N*) in the pycnocline (c). The white line depicts an interpolation between the points of maximum EC. Dashed red lines (in a and c) depict the parameter combinations at which the angle of the topography equals the angle of the internal tide beam ('critical' steepness). Black dashed lines indicate the parameter values for which we carried out simulations. In panel a, we plotted the mean slope (as calculated by Eq. (6)), for easy comparison with the realistic simulations, causing a gap. Note that the y-axes begin at 0.2 km depth because the figures depict EC on the continental slope and in our idealized simulation setting the minimum water depth is 200 m.

3.2 Realistic simulation setting

To investigate how the relationships between depth of internal-tide generation and slope steepness, latitude, and stratification turn out to be in a realistic setting, we simulated internal-tide generation using 84 continental slope transects with realistic seasonal stratification (Fig. 3). We plotted the average EC at the model seafloor based on available data on depth, slope steepness, and latitude at the transects (Fig. 5), as in Fig. 4. With the smooth topography in the idealized simulation setting only one peak in EC was present, but in the realistic simulation setting multiple peaks in EC were often found. Since cold-water corals might benefit from a local peak in EC regardless of whether it is the largest peak on the continental slope, we identified all peaks in EC on transects and added all peaks to Fig. 5. We further plotted the weighted mean of depth, slope, and latitude of internal-tide generation for all oceans and seasons together, along with a trendline (Fig. 6a-b). Similarly, we plotted the depth at which corals occur (Fig. 6c-d), which will be discussed in the next section (3.3).

The depth at which EC peaks decreases with increasing slope steepness (Fig. 5a-d) and internal-tide generation generally occurs about 1 km deeper on slopes with a steepness of 0.05 than on near flat topography (Fig. 6a). In the realistic simulation setting, slope regions with a steepness >0.05 were unusual (only 1.1 % of all slope regions) and most EC peaks were on slope regions with a steepness <0.06. From the poles towards the equator EC intensifies and the depth at which EC peaks occur increases (Fig. 5e-h). Mean EC depth is shallowest near the poles and around 20 degrees North (~0.5 km depth), decreases to about 0.9 km depth near 40 degrees North and 30 degrees South and slightly increases to 0.7 km depth near 20 degrees South and at the equator (Fig. 6b). EC seems somewhat shallower in summer than winter, but overall a seasonal effect is not evident (Fig. 5 and 6).

These relationships between the depth of internal-tide generation and two of the three main factors determining that depth of maximum generation allow for a comparison to the depth of coral occurrences.

https://doi.org/10.5194/egusphere-2023-941
Preprint. Discussion started: 11 May 2023
© Author(s) 2023. CC BY 4.0 License.

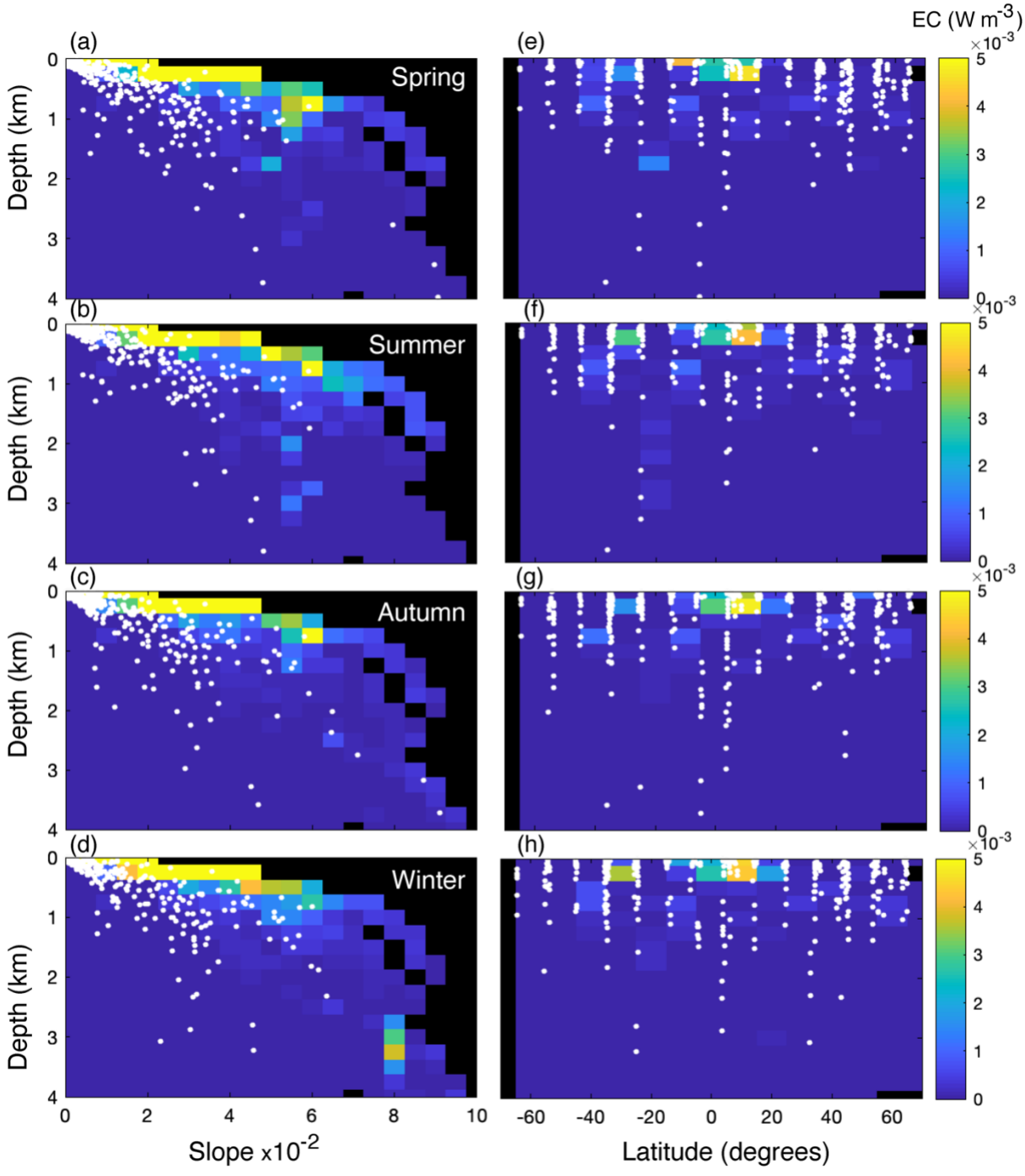

Figure 5. Colours depict average simulated energy conversion rates at the seafloor (W m^{-3}) for different values of slope steepness (a-d) and latitude (e-h). Simulations were performed with stratification profiles typical of Northern Hemisphere spring (a & e), summer (b & f), autumn (c & g), and winter (d & h). Black areas denote parameter combinations that were not present in any of the simulated transects. White dots show peaks in scaled EC.

https://doi.org/10.5194/egusphere-2023-941
Preprint. Discussion started: 11 May 2023
© Author(s) 2023. CC BY 4.0 License.

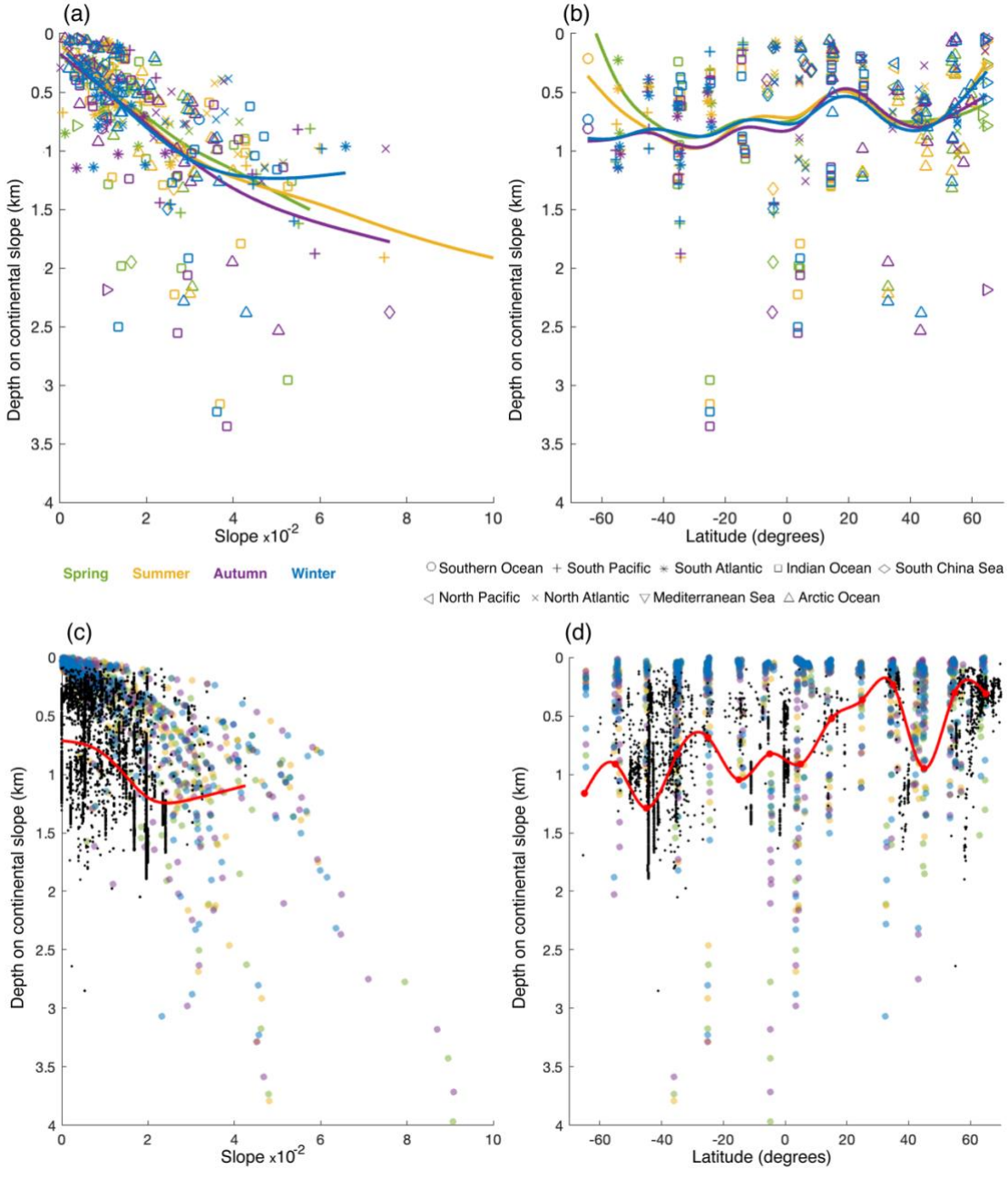

Figure 6. (a) Weighted mean depth of internal-tide generation against weighted mean slope steepness. (b) Weighted mean depth of internal-tide generation against weighted mean latitude. Colours depict the different seasons and symbols the different oceans. Lines depict a smoothing spline through the data from Northern Hemisphere spring (green), summer (yellow), autumn (purple), and winter (blue). (c) Depth at which cold-water corals occur (black dots) against slope steepness. The red line is a smoothing spline through the coral data to indicate the general trend. (d) relationship between the depth at which cold-water corals occur and latitude. The red line is a smoothing spline through a moving median (red dots), showing the general trend. A smoothing spline was fit through a moving average because it failed to fit through to the many observations at similar latitudes. Coloured dots in the background represent the EC peaks (as in Fig. 5), where the colours indicate the (NH) seasons. Coral occurrences are only included from regions where the tide is semidiurnal or mixed but mainly semidiurnal (as in Fig. 2).

https://doi.org/10.5194/egusphere-2023-941
Preprint. Discussion started: 11 May 2023
© Author(s) 2023. CC BY 4.0 License.

3.3 Coral occurrences

To investigate the effect of internal-tide generation on the occurrence of cold-water corals, we used several global databases with cold-water coral occurrences. Mapping the depth at which cold-water corals are found (Fig. 7) indicates that corals typically occur shallower near Norway, the Mediterranean Sea, the US west coast, and north Australia, and deeper in the open ocean (Atlantic and Pacific Ocean) than on continental slopes, except for Portugal and south of Australia. In some regions with cold-water occurrences, mainly the Mediterranean Sea, the Gulf of Mexico, the South China Sea, and South of Australia, the M2 barotropic (surface) tidal speed is <1 cm s^{-1}. In these areas the barotropic tidal signal is mainly diurnal (Fig. 2) and the influence of the internal M2 tide will therefore be limited.

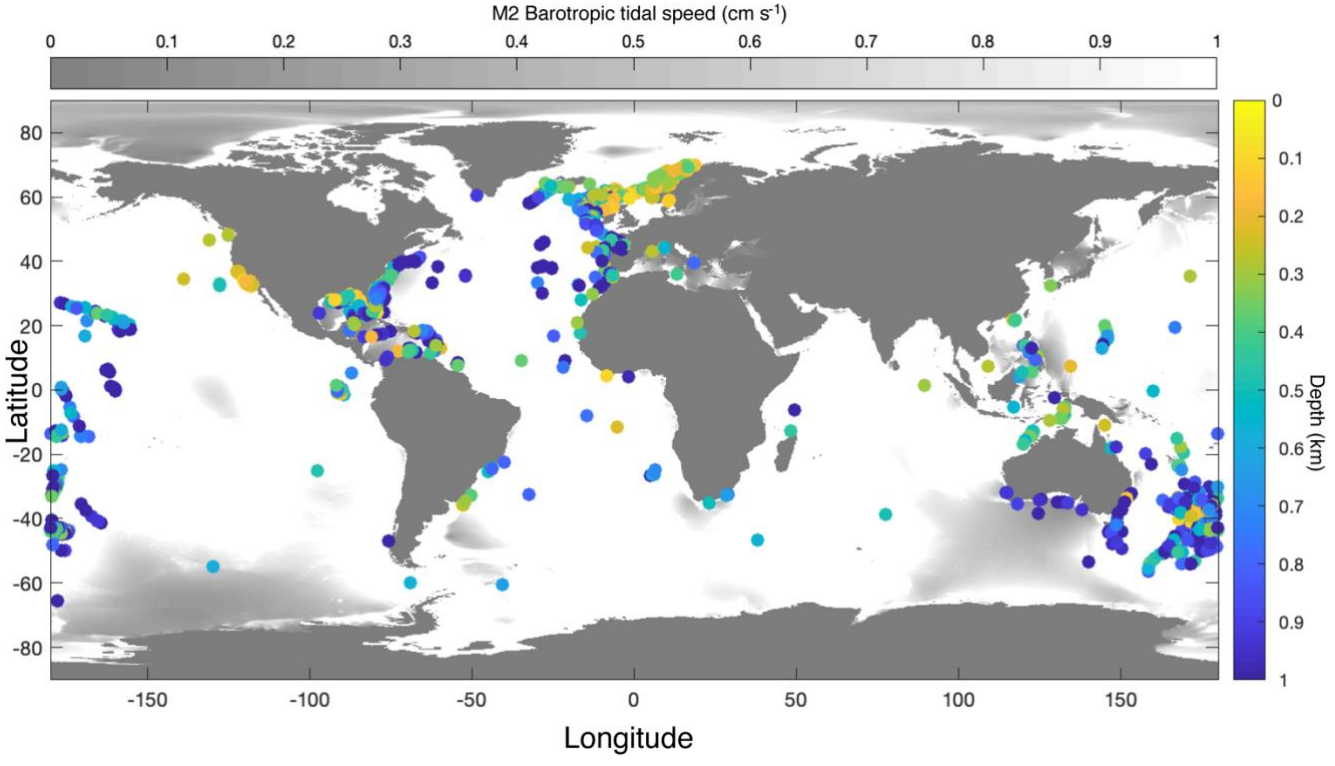

Figure 7. Map with all coral occurrences from the databases with colour indicating the depth at which the corals were found. In the oceans, grey shading indicates where the speed of the barotropic M2 tide is below 1 cm s-1. This map was created using the TPXO9 atlas (Egbert and Erofeeva, 2002).

With increasing slope steepness, the depth at which cold-water corals occur typically decreases, especially for slopes with a steepness <0.03, from about 0.7 km depth to 1.3 km depth (Fig. 6c). The depth at which cold-water corals occur is shallowest towards the northern pole and around 30 degrees North (~0.3 km depth) and deepest around 40 degrees South (~1.2 km depth; Fig. 6d). The depth at which corals occur decreases to about 0.7 km depth around 30 degrees South and increases towards 1 km depth near the equator. Towards the southern pole an outlier brings the average coral depth down towards about 1 km

https://doi.org/10.5194/egusphere-2023-941
Preprint. Discussion started: 11 May 2023
© Author(s) 2023. CC BY 4.0 License.

depth, but for the rest, the relationship is rather similar to the relationship between the depth of mean EC and latitude (Fig. 6b), both qualitatively (the trend) and quantitatively (the depths).

Besides a general comparison globally, we also compared the depth of peaks in internal-tide generation and the occurrence of cold-water corals on the 17 transects where cold-water corals occurred on or very nearby the transect (Fig. 8). We included only those transects in regions where the tide is semidiurnal or mixed but mainly semidiurnal and used scaled EC since cold-water corals might benefit from a peak in EC regardless of the intensity of that peak. On transects 6, 9, 20, 33, 90, 105, 114, 115, and 116, the depth at which cold-water corals are found coincides with the depth of a peak in EC in winter, and on transects 11, 13, 90, and 114 coral depth coincides with an EC peak in spring. On transect 18 the corals occur at the depth of increased EC regardless of season. On transects 51, and 91 corals occur within 200 m depth of increased EC as simulated by our model and on transects 17, 18, 52, and 106 there are corals occurring >600 m depth from increased EC. Cold-water corals occur often near peaks in internal-tide generation, but the relation between cold-water corals and internal-tide generation as found on a global scale is not necessarily indicative for coral occurrences at an individual level.

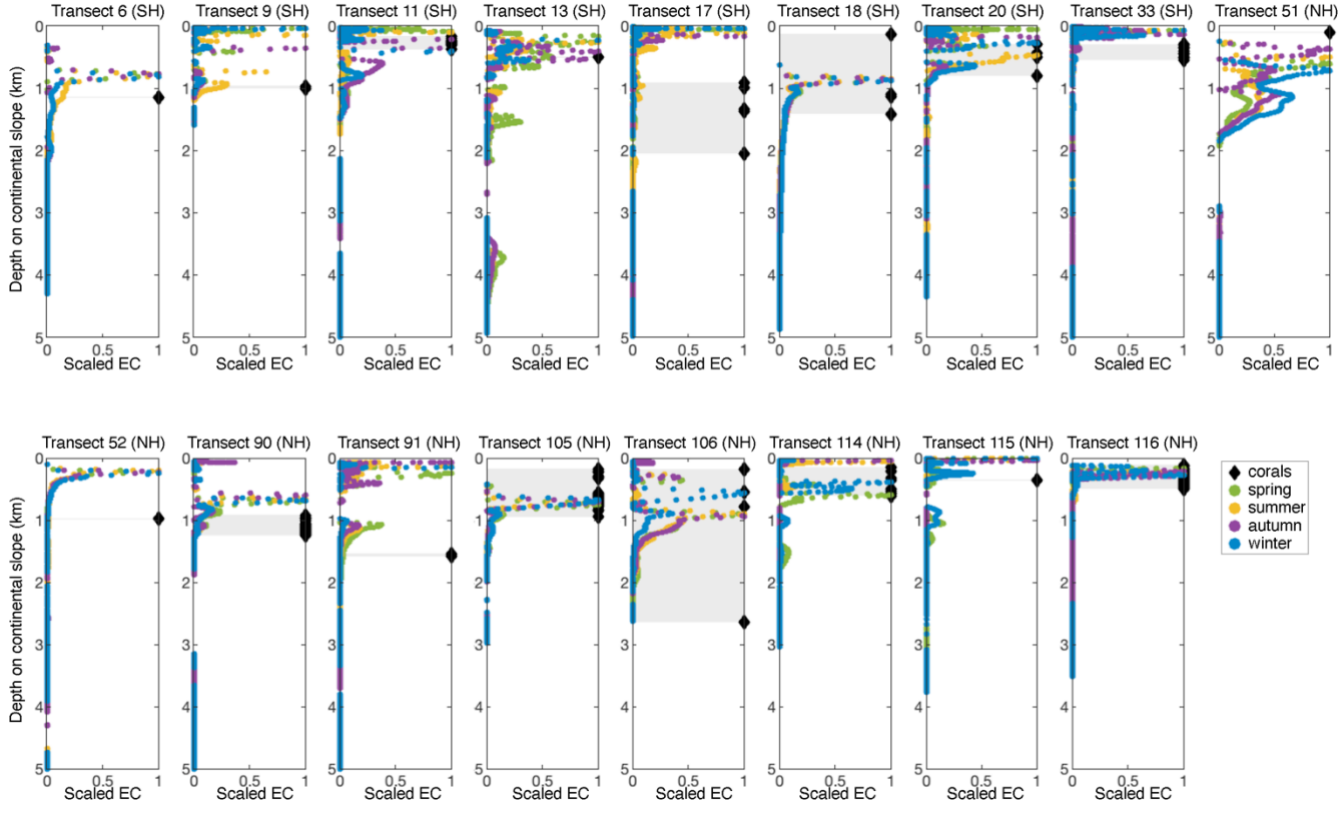

Figure 8. Scaled energy conversion to the internal tide (EC) on the model seafloor of 17 transects with overlapping cold-water coral occurrences in regions where the tide is semidiurnal or mixed but mainly semidiurnal (as in Fig. 2). Titles indicate the transect number and whether it is located on the Southern Hemisphere (SH) or Northern Hemisphere (NH). Shaded areas indicate the region connecting coral occurrences. Note that the season indication refers to NH seasons.

https://doi.org/10.5194/egusphere-2023-941
Preprint. Discussion started: 11 May 2023
© Author(s) 2023. CC BY 4.0 License.

4. Discussion

4.1 Slope steepness and the role of critical slopes for cold-water corals

We found that, for continental slopes with an average steepness <0.05, the depth of internal-tide generation decreases markedly with increasing slope steepness, with differences of a kilometre or more. Our idealized simulations show a reversal of this relationship for slopes with a steepness >0.06, but in reality, only few continental slopes were >0.05 on average. So, we conclude that a general steepening of the continental slope will likely decrease the depth of internal-tide generation and that the only few regions on continental slopes are (super)critical.

The amount of energy in the internal tide at the seafloor depends on the steepness of the topography compared to the steepness of the internal tidal beam (Fig. 1). At subcritical topography, the energy in the internal tide travels away from the topography to be dissipated in the interior of the ocean (de Lavergne et al., 2019; Gerkema, 2019; st. Laurent & Garrett, 2002). At critical topography, the energy in the internal tide is concentrated on the seafloor, giving rise to high amplitude waves and turbulence (Cacchione et al., 2002; Gerkema, 2019). At 'supercritical' topography, the energy contained in the internal tide is increased as compared to subcritical topography (Fig. 5a&c; Garrett & Kunze, 2006; Nash et al., 2004). Indeed, the percentage of (super)critical topography is much higher on those transect regions where we identified peaks in energy conversion (EC) to the M2 internal tide than generally on all transect regions (Fig. 9).

https://doi.org/10.5194/egusphere-2023-941
Preprint. Discussion started: 11 May 2023
© Author(s) 2023. CC BY 4.0 License.

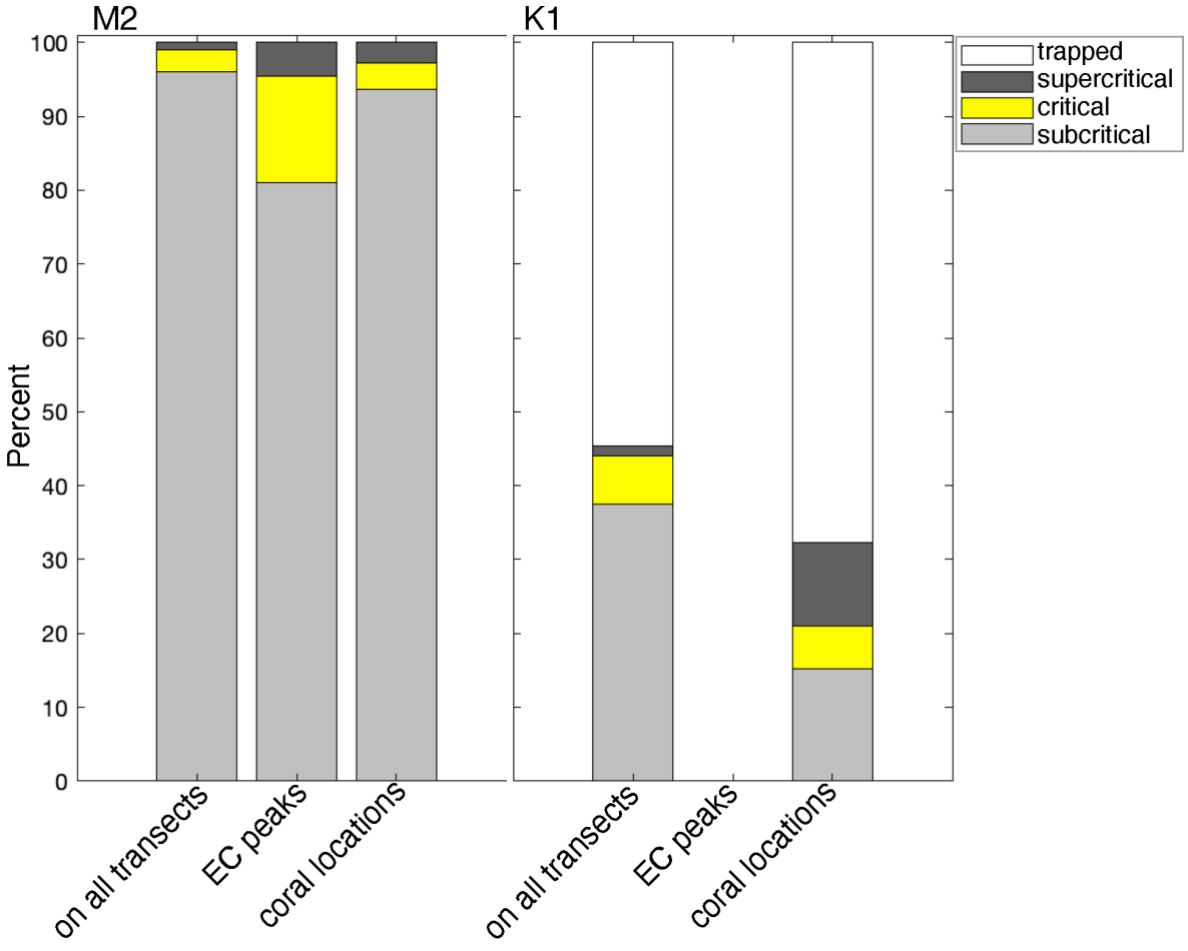

Figure 9. Bars show the percentage of slope regions where the internal tide is trapped at the topography (white sections), supercritical (dark grey), critical (yellow), or subcritical (light grey), for the M2 (left panel) or K1 (right panel) internal tide. From left to right, the bars show the percentages of all slope regions on all transects, slope regions with EC peaks, and locations of coral occurrences. We defined 'critical' as a region on the continental slope where the steepness of the topographic slope equals the angle of the internal tidal beam ± $5x10^{-7}$. When the Coriolis frequency equals the tidal frequency, the internal tide does not propagate, i.e., is trapped at the topography.

Cold-water corals generally seem to occur deeper on steeper continental slopes (Fig. 6c) and cold-water corals were often located close to EC peaks (Fig. 8). The increased dynamics from the reflection of internal tides on (super)critical topography would especially benefit benthic life. We here show that, like at the SE Rockall Bank margin (Frederiksen et al., 1992; Mohn et al., 2014), cold-water corals globally occur more often on topography that is (super)critical to the M2 or K1 internal tide (6.3 % and 17.5 % resp.) than what would be expected based on the percentage of (super)critical topography on all transects (4.0 % and 7.8 % for the M2 and K1 tide resp.; Fig. 9).

The internal K1 tide is trapped at the topography poleward of the critical latitude of 30 degrees. Interestingly, our data compilation shows that cold-water corals also occur more often at locations where the K1 internal tide is trapped at the

https://doi.org/10.5194/egusphere-2023-941
Preprint. Discussion started: 11 May 2023
© Author(s) 2023. CC BY 4.0 License.

topography (67.9 %; Fig. 9), than what would be expected based on the percentage of trapped K1 internal tide on all transects (54.7 %). Trapped internal tides have been associated to thick benthic boundary layers (Pereira et al., 2002) and increased surface productivity (Wilson, 2011), attributed to increased vertical mixing and turbulence around near critical latitudes (Robertson et al., 2017; Wilson, 2011; Gerkema and Shrira, 2005). At the SE Rockall Bank margin cold-water coral reefs are though to benefit from an internal tide at diurnal frequency because it is trapped at the topography there (Cyr et al., 2016; van Haren et al., 2014). Trapped internal tides are thus an interesting hydrodynamic mechanism that likely increases the food supply towards cold-water coral reefs which is not yet often considered in studies on cold-water coral food supply mechanisms.

4.2 Latitude and the role of stratification for cold-water corals

Our idealized simulations show that internal-tide generation deepens by several hundred meters from the poles towards the equator (Fig. 4b). With realistic topography and stratification, the depth at which the internal tide is generated is also shallowest near the poles and deepens by several hundred meters towards the equator, but then shoals around 20 degrees North and South (Fig. 6b). This difference between the theoretical and realistic simulations is likely caused by stratification, which is latitude-dependent (Fig. 10, note that slope is not correlated to latitude). Our idealized simulations show that stronger uniform stratification decreases the depth at which the internal tide is generated (Fig. 4c), but the effect of a seasonal and permanent pycnocline on the depth of internal-tide generation remains unclear.

A modelling study from the Bay of Biscay sheds light on the effect of seasonal stratification on internal-tide generation (Gerkema et al., 2004). The presence of a seasonal pycnocline in the top 50 m during summer increased internal-tide generation near the ocean surface whereas the continuous presence of the permanent pycnocline around 0.8 km depth increased internal-tide generation between 0.6 km to 1.4 km depth. Internal tidal waves propagate on the surface of isopycnals, so enhanced stratification increases the generation of internal tides at the depth of the pycnocline (Gerkema, 2019; Juva et al., 2020; Legg and Klymak, 2008). A shallow seasonal pycnocline thus decreases the mean depth at which internal tides are generated whereas deep stratification increases it. So, strong permanent stratification around 200 m depth, between 15 degrees South and 20 degrees North (Fig. 10), likely causes internal tides to be generated shallower on the continental margin. Seasonal stratification is stronger north than south of the equator (Fig. 10b-c), likely explaining why internal-tide generation is shallower north than south of the equator.

https://doi.org/10.5194/egusphere-2023-941
Preprint. Discussion started: 11 May 2023
© Author(s) 2023. CC BY 4.0 License.

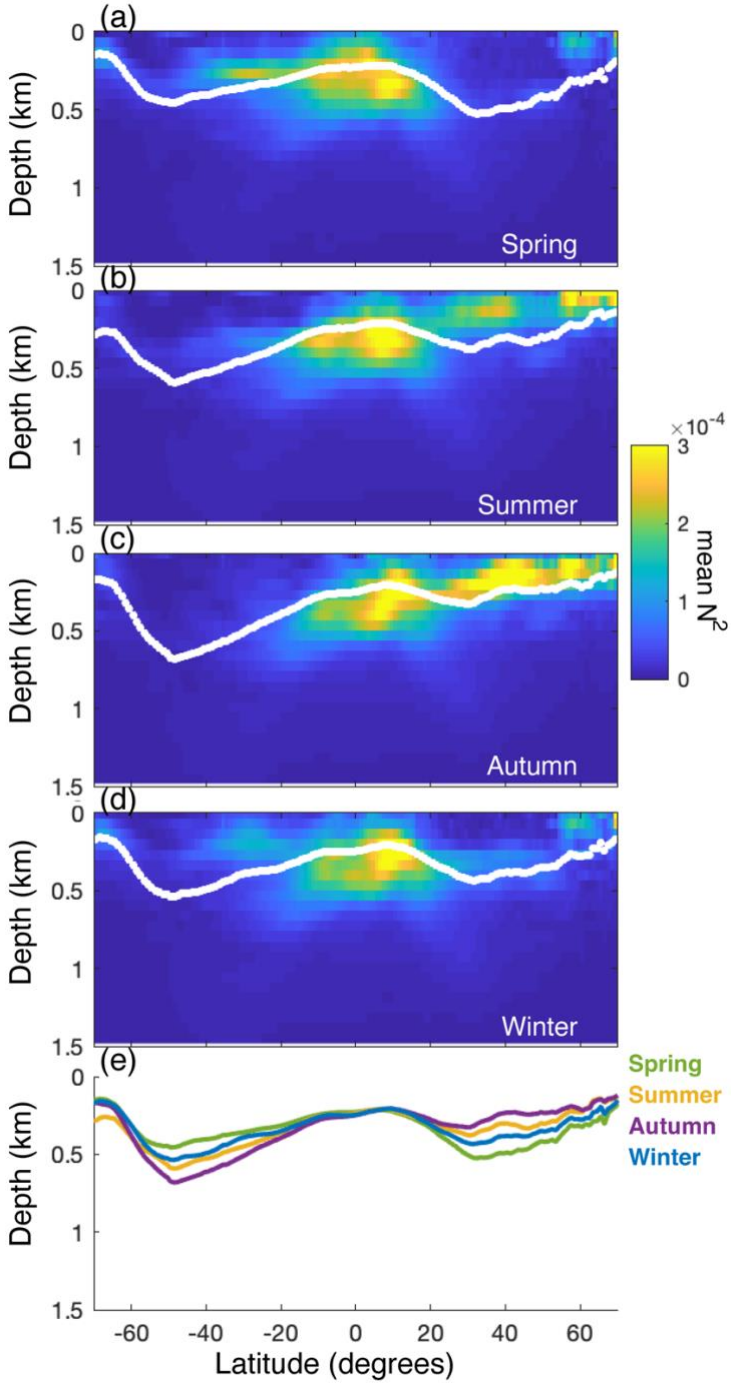

Figure 10. Intensity of stratification (N^2; calculated from the Levitus database) through the water column for every latitudinal degree, averaged over every longitudinal degree for (a) February-April ('spring'), (b) May-July ('summer'), (c) August-October ('autumn'), and (d) November-January ('winter'). White dots depict the weighted mean depth (Eq. (6) but weighted by stratification instead of energy conversion rate). (e) The relationship of the weighted mean depth of stratification against latitude in spring (green), summer (yellow), autumn (purple), and winter (blue).

https://doi.org/10.5194/egusphere-2023-941
Preprint. Discussion started: 11 May 2023
© Author(s) 2023. CC BY 4.0 License.

For the Rockall Bank margin, where cold-water corals grow on mounds of several hundred meters high, White & Dorschel (2010) argue that the permanent pycnocline controls the depth at which cold-water corals occur because of enhanced tidal currents in the pycnocline. The depth of the permanent pycnocline also represents the lower limit of deep winter mixing (Holliday et al., 2000). Other studies between 23 degrees North and 54 degrees North also highlight the importance of a deep pycnocline for cold-water coral growth and coral mound development (Rüggeberg et al., 2016; Wienberg et al., 2020; Matos et al., 2017; Wang et al., 2019). We here show that cold-water corals globally show a depth-pattern (Fig. 6d) that is similar as the depth-pattern of stratification (Fig. 10) and that this can be related to the depth of internal-tide generation (Fig. 6b)

4.3 Internal tides and other food supply mechanisms for cold-water corals

While we focussed only on internal-tide generation at continental slopes, cold-water coral growth might also be stimulated at great depths by internal waves generated in the open ocean (Fig. 7); this would be expected to occur at rough topography on the boundaries of water masses at depths beyond the stratification profiles used in our simulations (Nikurashin and Ferrari, 2013). However, most coral observations were located within the maximum depth of our stratification profiles, i.e., 1.45 km depth (Fig. 6c-d). So, our simulations seem to capture the most important features of internal-tide generation for cold-water corals on continental slopes. Internal-tide generation thus likely facilitates or even determines cold-water coral occurrence in most locations (this paper; Juva et al., 2020).

Indeed, we showed that, overall, the depth-pattern of coral occurrences is similar to that of internal-tide generation, but with a considerable spread. Slope steepness has a larger effect on the depth of internal-tide generation than latitude (Fig. 6a-b), which can be one explanation for the large spread in the depths of internal-tide generation and cold-water coral occurrences. Many other site-specific food supply mechanisms have also been described that could weaken the association of cold-water corals to internal tides.

Trapped internal tides can also be beneficial for cold-water corals (section 4.1; Cyr et al., 2016; van der Kaaden et al., 2021; van Haren et al., 2014) but the mechanism of their generation has not yet been studied and is beyond the scope of the model used in this paper. Trapped internal tide might occur at different depths, possibly stimulating cold-water coral growth at a different depth.

High surface productivity has also been found as a factor controlling cold-water coral growth (White et al., 2005; Eisele et al., 2011; Fink et al., 2013; Wienberg et al., 2022) in which case cold-water corals might be able to survive at greater depths. For cold-water coral reefs within a few hundred meters from the ocean surface (e.g., Norwegian reefs), wind-induced Ekman transport is likely an important food supply mechanism (Thiem et al., 2006). Furthermore, the formation of nepheloid layers (Mienis et al., 2007, 2012) and the presence of specific water masses (Schulz et al., 2020; Dullo et al., 2008) have been mentioned as environmental drivers of cold-water coral occurrence.

Cold-water coral reefs further often develop into cold-water coral mounds when reef growth and sediment supply are sufficient (van der Land et al., 2014; Wang et al., 2021; Pirlet et al., 2011). Most mounds are some tens of meter high (Freiwald, 2002), but some can become several hundred meters high (Wheeler et al., 2007), so over time, cold-water corals actively decrease the

https://doi.org/10.5194/egusphere-2023-941
Preprint. Discussion started: 11 May 2023
© Author(s) 2023. CC BY 4.0 License.

depth at which they occur. Already from some tens of meters high (van der Kaaden et al., 2021), such coral structures have a major effect on their environment, likely increasing their own food supply and possibly surmounting the environmental control from ambient environmental processes such as internal-tide generation (van der Kaaden et al., 2021; Soetaert et al., 2016). So, the depth of internal-tide generation therefore most likely determines the depth of cold-water coral mound initiation (van der Kaaden et al., 2021; Wang et al., 2019; Wienberg et al., 2020), which might be several tens to hundreds of meters below the current depth of coral occurrence.

5. Conclusion and outlook

Cold-water coral reefs are highly productive ecosystems in the deep-sea that benefit from mechanisms enhancing the vertical transport of high-quality organic matter from near the ocean surface (da Costa Portilho-Ramos et al., 2022; Snelgrove et al., 2017; Cathalot et al., 2015). Internal tides are beneficial for cold-water coral reef and mound formation because they accelerate the vertical transport of organic matter from near the ocean surface towards the seafloor (de Froe et al., 2022; Mohn et al., 2014; Frederiksen et al., 1992; Davies et al., 2009). Previous studies suggested that the region on the continental slope where internal tides are generated is especially important for cold-water corals (van der Kaaden et al., 2021).

We found that the relationship between the depth of internal-tide generation and continental slope steepness and latitude is very similar to that of deep-sea reef building coral occurrences, in their functional dependence on slope steepness and latitude. To our knowledge, this is the first time that the global relationships between the depth of internal-tide generation and the three parameters governing internal-tide generation have been elucidated and that the connection of internal tides to cold-water coral occurrences has been made on a global scale.

Most continental slopes in the ocean are rather gentle (<0.05 steepness), and for this range the depth of internal-tide generation decreases with increasing slope steepness. From the poles towards the equator internal-tide generation typically deepens, but strong seasonal stratification around 25 degrees North and South and strong permanent stratification near the equator cause a shoaling of internal-tide generation. Slope steepness has a larger effect on the depth of internal-tide generation than latitude, but the effect of latitude is considerable.

The depth-pattern of internal-tide generation and latitude is remarkably similar to the depth-pattern of cold-water corals, and on transects cold-water corals are often found at peaks of internal-tide generation. We conclude that there is a relation between the depth at which cold-water corals occur and the depth of internal-tide generation globally. We here also showed that cold-water corals are more often than randomly associated to trapped (diurnal) internal tides, highlighting trapped internal tides as an interesting potential food supply mechanism to cold-water corals, which deserves further study but falls outside the scope of the model used here. We show that it is important to consider the depth of internal-tide generation on continental margins, especially in studies relating internal waves to benthic life, for example in habitat suitability models.

Climate change will likely increase stratification globally (Reid et al., 2009; Li et al., 2018; Capotondi et al., 2012), which, based on our study, will likely cause a shoaling of internal-tide generation on continental slopes. So, with a warming of the climate, new suitable habitat for cold-water coals might be created shallower on continental slopes. Since warmer temperatures

https://doi.org/10.5194/egusphere-2023-941
Preprint. Discussion started: 11 May 2023
© Author(s) 2023. CC BY 4.0 License.

increase the energy demand of cold-water corals (Dodds et al., 2007; Dorey et al., 2020; Chapron et al., 2021), suitable cold-water coral habitat is expected to deepen in a warmer climate (Morato et al., 2020). A sufficient food supply to cold-water corals can however compensate adverse environmental conditions to some degree (da Costa Portilho-Ramos et al., 2022; Hebbeln et al., 2020; Dorey et al., 2020; Büscher et al., 2017). Wienberg et al. (2020) similarly found (for the Belgica cold-water coral mound province) that cold-water coral growth followed a shoaling of the region of internal wave activity, which they linked to water mass boundaries. Since at shallower depths coral food supply is higher, the creation of new suitable habitat at shallower regions on continental slopes might provide a mechanism whereby cold-water corals can compensate the higher energetic costs from warmer temperatures.

Appendix A

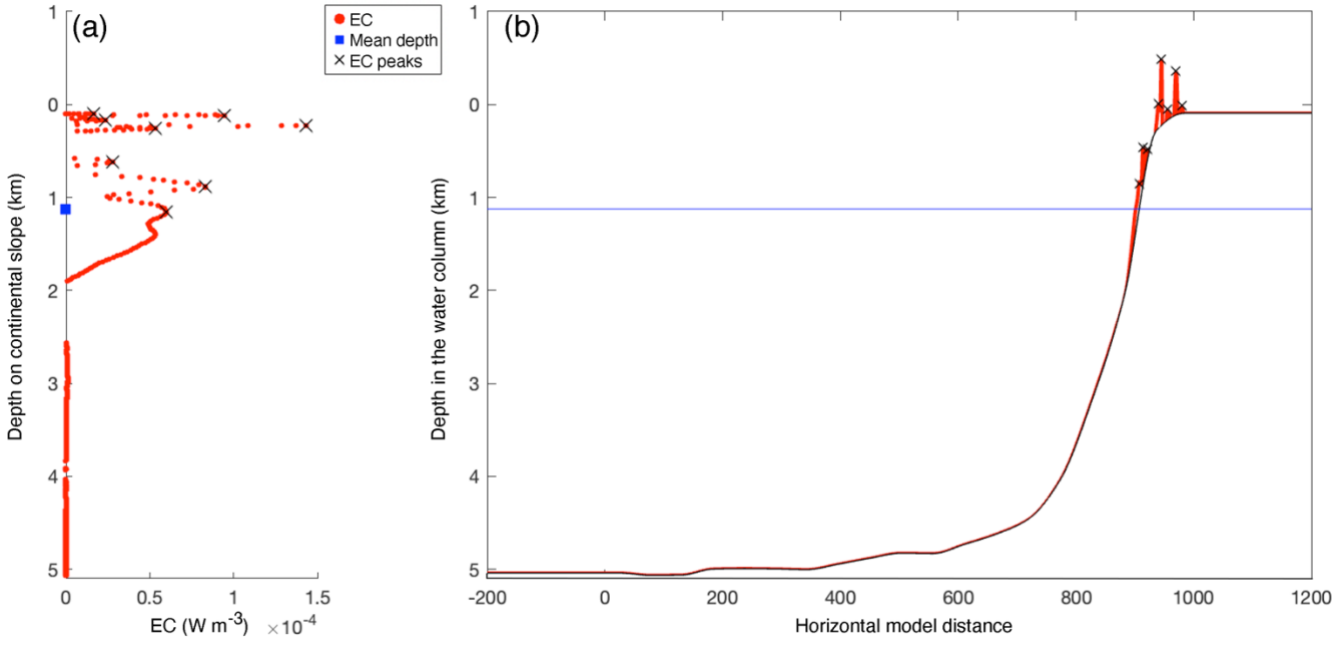

Figure A1. Example of energy conversion rates (EC) at the model seafloor on transect 12 (the 'winter' simulation), with peaks as identified by Matlabs peaks-finding algorithm and weighted mean depth as calculated by Eq. (6). (a) energy conversion rate (red) on the continental slope. Black crosses indicate peaks in EC and the blue square indicates the weighted mean depth as calculated by Eq. (6). The y-axis denotes the depth on the continental slope, i.e., *z* in Eq. (6). (b) energy conversion rate (red) plotted on the transect topography (black). Black crosses indicate peaks in EC and the blue line indicates the weighted mean depth. The y-axis denotes the depth through the water column.

Code availability

The internal tide model has been described in detail in Gerkema et al. (2004) and succinctly in the methods section of this paper. The model code can be made available on request.

https://doi.org/10.5194/egusphere-2023-941
Preprint. Discussion started: 11 May 2023
© Author(s) 2023. CC BY 4.0 License.

Data availability

Data on cold-water coral occurrences were obtained from the following open databases and used as described in the methods section of this paper: the NOAA National Database for Deep-sea Corals and Sponges (NOAA National Database for Deep-Sea Corals and Sponges, version 20220426-0), ICES Vulnerable Marine Ecosystems (International Council for the Exploration of the Sea, June 2022) and OBIS (OBIS, 2022).

Author contributions

AvdK, DvO, and TG were involved in the conceptualization of the study. The work was supervised by DvO and TG. The model used was developed by TG. The study was executed, and the results were written by AvdK. DvO, JvdK, KS, and MR secured funding for the project. All co-authors commented on the final draft of the manuscript.

Competing interests

The authors declare that they have no conflict of interest.

Acknowledgements

We thank Emil Sigmann Engh for constructing the database of cold-water coral occurrences. This research has been made possible with collaboration funding between the Royal Dutch Institute for Sea Research and Utrecht University. CM has received funding from the European Horizon 2020 Research and Innovation Programme under grant agreement no. 818123 (iAtlantic). The output of this study reflects only the author's view, and the European Union cannot be held responsible for any use that may be made of the information contained therein.

References

Banyte, D., Smeed, D. A., and Morales Maqueda, M.: The Weakly Stratified Bottom Boundary Layer of the Global Ocean, J Geophys Res Oceans, 123, 5587–5598, https://doi.org/10.1029/2018JC013754, 2018.

Büscher, J. V., Form, A. U., and Riebesell, U.: Interactive effects of ocean acidification and warming on growth, fitness and survival of the cold-water coral Lophelia pertusa under different food availabilities, Front Mar Sci, 4, https://doi.org/10.3389/fmars.2017.00101, 2017.

Cacchione, D. A., Pratson, L. F., and Ogston, A. S.: The Shaping of Continental Slopes by Internal Tides, Science (1979), 296, 724–727, https://doi.org/10.1126/science.1069803, 2002.

https://doi.org/10.5194/egusphere-2023-941
Preprint. Discussion started: 11 May 2023
© Author(s) 2023. CC BY 4.0 License.

Capotondi, A., Alexander, M. A., Bond, N. A., Curchitser, E. N., and Scott, J. D.: Enhanced upper ocean stratification with climate change in the CMIP3 models, J Geophys Res, 117, 1–23, https://doi.org/10.1029/2011JC007409, 2012.

Carlier, A., Le Guilloux, E., Olu, K., Sarrazin, J., Mastrototaro, F., Taviani, M., and Clavier, J.: Trophic relationships in a deep Mediterranean cold-water coral bank (Santa Maria di Leuca, Ionian Sea), Mar Ecol Prog Ser, 397, 125–137, https://doi.org/10.3354/meps08361, 2009.

Cathalot, C., Van Oevelen, D., Cox, T. J. S., Kutti, T., Lavaleye, M., Duineveld, G., and Meysman, F. J. R.: Cold-water coral reefs and adjacent sponge grounds: hotspots of benthic respiration and organic carbon cycling in the deep sea, Front Mar Sci, 2, 1–12, https://doi.org/10.3389/fmars.2015.00037, 2015.

Chapron, L., Galand, P. E., Pruski, A. M., Peru, E., Vétion, G., Robin, S., and Lartaud, F.: Resilience of cold-water coral holobionts to thermal stress, Proceedings of the Royal Society B: Biological Sciences, 288, https://doi.org/10.1098/rspb.2021.2117, 2021.

da Costa Portilho-Ramos, R., Titschack, J., Wienberg, C., Rojas, M. G. S., Yokoyama, Y., and Hebbeln, D.: Major environmental drivers determining life and death of cold-water corals through time, PLoS Biol, 20, https://doi.org/10.1371/journal.pbio.3001628, 2022.

Cyr, F., Van Haren, H., Mienis, F., Duineveld, G., and Bourgault, D.: On the influence of cold-water coral mound size on flow hydrodynamics, and vice versa, Geophys Res Lett, 43, 1–9, https://doi.org/10.1002/2015GL067038, 2016.

Davies, A. J., Duineveld, G. C. A., Lavaleye, M. S. S., Bergman, M. J. N., van Haren, H., and Roberts, J. M.: Downwelling and deep-water bottom currents as food supply mechanisms to the cold-water coral Lophelia pertusa (Scleractinia) at the Mingulay Reef complex, Limnol Oceanogr, 54, 620–629, https://doi.org/10.4319/lo.2009.54.2.0620, 2009.

Dodds, L. A., Roberts, J. M., Taylor, A. C., and Marubini, F.: Metabolic tolerance of the cold-water coral Lophelia pertusa (Scleractinia) to temperature and dissolved oxygen change, J Exp Mar Biol Ecol, 349, 205–214, https://doi.org/10.1016/j.jembe.2007.05.013, 2007.

Dorey, N., Gjelsvik, Ø., Kutti, T., and Büscher, J. V.: Broad Thermal Tolerance in the Cold-Water Coral Lophelia pertusa From Arctic and Boreal Reefs, Front Physiol, 10, https://doi.org/10.3389/fphys.2019.01636, 2020.

Dullo, W. C., Flögel, S., and Rüggeberg, A.: Cold-water coral growth in relation to the hydrography of the Celtic and Nordic European continental margin, Mar Ecol Prog Ser, 371, 165–176, https://doi.org/10.3354/meps07623, 2008.

Egbert, G. D. and Erofeeva, S. Y.: Efficient inverse modeling of barotropic ocean tides, J Atmos Ocean Technol, 19, 183–204, https://doi.org/10.1175/1520-0426(2002)019<0183:EIMOBO>2.0.CO;2, 2002.

Eisele, M., Frank, N., Wienberg, C., Hebbeln, D., López Correa, M., Douville, E., and Freiwald, A.: Productivity controlled cold-water coral growth periods during the last glacial off Mauritania, Mar Geol, 280, 143–149, https://doi.org/10.1016/j.margeo.2010.12.007, 2011.

van Engeland, T., Rune Godø, O., Johnsen, E., Duineveld, G. C. A., and van Oevelen, D.: Cabled ocean observatory data reveal food supply mechanisms to a cold-water coral reef, Prog Oceanogr, 172, 51–64, https://doi.org/10.1016/j.pocean.2019.01.007, 2019.

https://doi.org/10.5194/egusphere-2023-941
Preprint. Discussion started: 11 May 2023
© Author(s) 2023. CC BY 4.0 License.

Fink, H. G., Wienberg, C., de Pol-Holz, R., Wintersteller, P., and Hebbeln, D.: Cold-water coral growth in the Alboran Sea related to high productivity during the Late Pleistocene and Holocene, Mar Geol, 339, 71–82, https://doi.org/10.1016/j.margeo.2013.04.009, 2013.

Frederiksen, R., Jensen, A., and Westerberg, H.: The distribution of the scleractinian coral Lophelia pertusa around the Faroe islands and the relation to internal tidal mixing, Sarsia, 77, 157–171, https://doi.org/10.1080/00364827.1992.10413502, 1992.

Freiwald, A.: Reef-Forming Cold-Water Corals, in: Ocean margin Systems, 365–385, https://doi.org/10.1016/B978-012374473-9.00666-4, 2002.

Freiwald, A., Fosså, J. H., Grehan, A., Koslow, T., and Roberts, J. M.: Cold-water coral reefs: Out of sight – no longer out of mind, UNEP-WCMC, Cambridge, UK, https://doi.org/10.1016/j.dsr.2008.04.010, 2004.

de Froe, E., Maier, S. R., Horn, H. G., Wolff, G. A., Blackbird, S., Mohn, C., Schultz, M., van der Kaaden, A., Cheng, C. H., Wubben, E., van Haastregt, B., Friis Moller, E., Lavaleye, M., Soetaert, K., Reichart, G., and van Oevelen, D.: Hydrography and food distribution during a tidal cycle above a cold-water coral mound, Deep-Sea Research Part I, 189, 103854, https://doi.org/10.1016/j.dsr.2022.103854, 2022.

Garrett, C. and Kunze, E.: Internal Tide Generation in the Deep Ocean, Annu Rev Fluid Mech, 39, 57–87, https://doi.org/10.1146/annurev.fluid.39.050905.110227, 2006.

Gerkema, T.: An Introduction to Tides, Cambridge University Press, https://doi.org/10.1017/9781316998793, 2019.

Gerkema, T. and Shrira, V. I.: Near-inertial waves in the ocean: Beyond the “traditional approximation,” J Fluid Mech, 529, 195–219, https://doi.org/10.1017/S0022112005003411, 2005.

Gerkema, T., Lam, F. P. A., and Maas, L. R. M.: Internal tides in the Bay of Biscay: Conversion rates and seasonal effects, Deep Sea Res 2 Top Stud Oceanogr, 51, 2995–3008, https://doi.org/10.1016/j.dsr2.2004.09.012, 2004.

Hanz, U., Wienberg, C., Hebbeln, D., Duineveld, G., Lavaleye, M., Juva, K., Dullo, W.-C., Freiwald, A., Tamborrino, L., Reichart, G.-J., Flögel, S., and Mienis, F.: Environmental factors influencing cold-water coral ecosystems in the oxygen minimum zones on the Angolan and Namibian margins, Biogeosciences Discussions, 1–37, https://doi.org/10.5194/bg-2019-52, 2019.

van Haren, H., Mienis, F., Duineveld, G. C. A., and Lavaleye, M. S. S.: High-resolution temperature observations of a trapped nonlinear diurnal tide influencing cold-water corals on the Logachev mounds, Prog Oceanogr, 125, 16–25, https://doi.org/10.1016/j.pocean.2014.04.021, 2014.

Hebbeln, D., Wienberg, C., Dullo, W. C., Freiwald, A., Mienis, F., Orejas, C., and Titschack, J.: Cold-water coral reefs thriving under hypoxia, Coral Reefs, 39, 853–859, https://doi.org/10.1007/s00338-020-01934-6, 2020.

Holliday, N. P., Pollard, R. T., Read, J. F., and Leach, H.: Water mass properties and fluxes in the Rockall Trough, 1975-1998, Deep Sea Res 1 Oceanogr Res Pap, 47, 1303–1332, https://doi.org/10.1016/S0967-0637(99)00109-0, 2000.

International Council for the Exploration of the Sea (16 June 2022): ICES Vulnerable Marine Ecosystems data portal. https://vme.ices.dk/download.aspx.

https://doi.org/10.5194/egusphere-2023-941
Preprint. Discussion started: 11 May 2023
© Author(s) 2023. CC BY 4.0 License.

Jackson, C., da Silva, J., and Jeans, G.: The Generation of Nonlinear Internal Waves, Oceanography, 25, 108–123, https://doi.org/10.5670/oceanog.2011.65, 2012.

Juva, K., Flögel, S., Karstensen, J., Linke, P., and Dullo, W.-C.: Tidal dynamics control on cold-water coral growth: A high-resolution multivariable study on eastern Atlantic cold-water coral sites, Front Mar Sci, 7, 132, https://doi.org/10.3389/FMARS.2020.00132, 2020.

van der Kaaden, A.-S., Mohn, C., Gerkema, T., Maier, S. R., de Froe, E., van de Koppel, J., Rietkerk, M., Soetaert, K., and van Oevelen, D.: Feedbacks between hydrodynamics and cold-water coral mound development, Deep-Sea Research Part I, 178, https://doi.org/10.1016/j.dsr.2021.103641, 2021.

van der Land, C., Eisele, M., Mienis, F., de Haas, H., Hebbeln, D., Reijmer, J. J. G., and van Weering, T. C. E.: Carbonate mound development in contrasting settings on the Irish margin, Deep Sea Res 2 Top Stud Oceanogr, 99, 297–306, https://doi.org/10.1016/j.dsr2.2013.10.004, 2014.

st. Laurent, L. and Garrett, C.: The Role of Internal Tides in Mixing the Deep Ocean, J Phys Oceanogr, 32, 2882–2899, https://doi.org/10.1175/1520-0485(2002)032<2882:TROITI>2.0.CO;2, 2002.

de Lavergne, C., Falahat, S., Madec, G., Roquet, F., Nycander, J., and Vic, C.: Toward global maps of internal tide energy sinks, Ocean Model (Oxf), 137, 52–75, https://doi.org/10.1016/j.ocemod.2019.03.010, 2019.

Legg, S. and Klymak, J.: Internal Hydraulic Jumps and Overturning Generated by Tidal Flow over a Tall Steep Ridge, J Phys Oceanogr, 38, 1949–1964, https://doi.org/10.1175/2008jpo3777.1, 2008.

Levitus, S. E.: Climatological atlas of the world ocean, NOAA Professional Paper 13, 1982.

Li, G., Cheng, L., Zhu, J., Trenberth, K. E., Mann, M. E., and Abraham, J. P.: Increasing ocean stratification over the past half-century, Nat Clim Chang, https://doi.org/10.1038/s41558-020-00918-2, 2018.

Matos, L., Wienberg, C., Titschack, J., Schmiedl, G., Frank, N., Abrantes, F., Cunha, M. R., and Hebbeln, D.: Coral mound development at the Campeche cold-water coral province , southern Gulf of Mexico : Implications of Antarctic Intermediate Water increased influence during interglacials, Mar Geol, 392, 53–65, https://doi.org/10.1016/j.margeo.2017.08.012, 2017.

Mienis, F., de Stigter, H. C., White, M., Duineveld, G., de Haas, H., and van Weering, T. C. E.: Hydrodynamic controls on cold-water coral growth and carbonate-mound development at the SW and SE Rockall Trough Margin, NE Atlantic Ocean, Deep Sea Res 1 Oceanogr Res Pap, 54, 1655–1674, https://doi.org/10.1016/j.dsr.2007.05.013, 2007.

Mienis, F., de Stigter, H. C., de Haas, H., van der Land, C., and van Weering, T. C. E.: Hydrodynamic conditions in a cold-water coral mound area on the Renard Ridge, southern Gulf of Cadiz, Journal of Marine Systems, 96, 61–71, https://doi.org/10.1016/j.jmarsys.2012.02.002, 2012.

Mohn, C., Rengstorf, A., White, M., Duineveld, G., Mienis, F., Soetaert, K., and Grehan, A.: Linking benthic hydrodynamics and cold-water coral occurrences: A high-resolution model study at three cold-water coral provinces in the NE Atlantic, Prog Oceanogr, 122, 92–104, https://doi.org/10.1016/j.pocean.2013.12.003, 2014.

Morato, T., González-Irusta, J. M., Dominguez-Carrió, C., Wei, C. L., Davies, A., Sweetman, A. K., Taranto, G. H., Beazley, L., García-Alegre, A., Grehan, A., Laffargue, P., Murillo, F. J., Sacau, M., Vaz, S., Kenchington, E., Arnaud-Haond, S.,

https://doi.org/10.5194/egusphere-2023-941
Preprint. Discussion started: 11 May 2023
© Author(s) 2023. CC BY 4.0 License.

Callery, O., Chimienti, G., Cordes, E., Egilsdottir, H., Freiwald, A., Gasbarro, R., Gutiérrez-Zárate, C., Gianni, M., Gilkinson, K., Wareham Hayes, V. E., Hebbeln, D., Hedges, K., Henry, L. A., Johnson, D., Koen-Alonso, M., Lirette, C., Mastrototaro, F., Menot, L., Molodtsova, T., Durán Muñoz, P., Orejas, C., Pennino, M. G., Puerta, P., Ragnarsson, S., Ramiro-Sánchez, B., Rice, J., Rivera, J., Roberts, J. M., Ross, S. W., Rueda, J. L., Sampaio, Í., Snelgrove, P., Stirling, D., Treble, M. A., Urra, J., Vad, J., van Oevelen, D., Watling, L., Walkusz, W., Wienberg, C., Woillez, M., Levin, L. A., and Carreiro-Silva, M.: Climate-induced changes in the suitable habitat of cold-water corals and commercially important deep-sea fishes in the North Atlantic, Glob Chang Biol, 26, 2181–2202, https://doi.org/10.1111/gcb.14996, 2020.

Nakatsuka, T., Handa, N., Harada, N., Sugimoto, T., and Imaizumi, S.: Origin and decomposition of sinking particulate organic matter in the deep water column inferred from the vertical distributions of its δ15N, δ13 and δ14, Deep Sea Research Part I: Oceanographic Research Papers, 44, 1957–1979, https://doi.org/10.1016/s0967-0637(97)00051-4, 1997.

Nash, J. D., Kunze, E., Toole, J. M., and Schmitt, R. W.: Internal Tide Reflection and Turbulent Mixing on the Continental Slope, 2004.

Nikurashin, M. and Ferrari, R.: Overturning circulation driven by breaking internal waves in the deep ocean, Geophys Res Lett, 40, 3133–3137, https://doi.org/10.1002/grl.50542, 2013.

NOAA National Database for Deep-Sea Corals and Sponges (version 20220426-0): https://deepseacoraldata.noaa.gov/; NOAA Deep Sea Coral Research & Technology Program.

NOAA National Geophysical Data Center: ETOPO1 1 Arc-Minute Global Relief Model., NOAA National Centers for Environmental Information., 2009.

OBIS: Ocean Biodiversity Information System. Intergovernmental Oceanographic Commission of UNESCO. www.obis.org, 2022.

van Oevelen, D., Duineveld, G. C. A., Lavaleye, M. S. S., Kutti, T., and Soetaert, K.: Trophic structure of cold-water coral communities revealed from the analysis of tissue isotopes and fatty acid composition, Marine Biology Research, 14, 287–306, https://doi.org/10.1080/17451000.2017.1398404, 2018.

Pante, E. and Simon-Bouhet, B.: marmap: A Package for Importing, Plotting, and Analyzing Bathymetric and Topographic Data in R, PLoS One, 8, https://doi.org/10.1371/journal.pone.0073051, 2013.

Pereira, A. F., Beckmann, A., and Hellmer, H. H.: Tidal Mixing in the Southern Weddell Sea: Results from a Three-Dimensional Model, 2002.

Pirlet, H., Colin, C., Thierens, M., Latruwe, K., Van Rooij, D., Foubert, A., Frank, N., Blamart, D., Huvenne, V. A. I., Swennen, R., Vanhaecke, F., and Henriet, J. P.: The importance of the terrigenous fraction within a cold-water coral mound: A case study, Mar Geol, 282, 13–25, https://doi.org/10.1016/j.margeo.2010.05.008, 2011.

Reid, P. C., Fischer, A. C., Lewis-Brown, E., Meredith, M. P., Sparrow, M., Andersson, A. J., Antia, A., Bates, N. R., Bathmann, U., Beaugrand, G., Brix, H., Dye, S., Edwards, M., Furevik, T., Gangstø, R., Hátún, H., Hopcroft, R. R., Kendall, M., Kasten, S., Keeling, R., Le Quéré, C., Mackenzie, F. T., Malin, G., Mauritzen, C., Ólafsson, J., Paull, C., Rignot, E.,

https://doi.org/10.5194/egusphere-2023-941
Preprint. Discussion started: 11 May 2023
© Author(s) 2023. CC BY 4.0 License.

Shimada, K., Vogt, M., Wallace, C., Wang, Z., and Washington, R.: Impacts of the Oceans on Climate Change, in: Advances in Marine Biology, vol. 56, 1–150, 2009.

Roberts, E., Bowers, D., Meyer, H., Samuelsen, A., Rapp, H., and Cárdenas, P.: Water masses constrain the distribution of deep-sea sponges in the North Atlantic Ocean and Nordic Seas, Mar Ecol Prog Ser, 659, 75–96, https://doi.org/10.3354/meps13570, 2021.

Robertson, R., Dong, J., and Hartlipp, P.: Diurnal Critical Latitude and the Latitude Dependence of Internal Tides, Internal Waves, and Mixing Based on Barcoo Seamount, J Geophys Res Oceans, 122, 7838–7866, https://doi.org/10.1002/2016JC012591, 2017.

Rüggeberg, A., Flögel, S., Dullo, W. C., Raddatz, J., and Liebetrau, V.: Paleoseawater density reconstruction and its implication for cold-water coral carbonate mounds in the northeast Atlantic through time, Paleoceanography, 31, 365–379, https://doi.org/10.1002/2015PA002859, 2016.

Sarkar, S. and Scotti, A.: From Topographic Internal Gravity Waves to Turbulence, Annu Rev Fluid Mech, 49, 195–220, https://doi.org/10.1146/annurev-fluid-010816-060013, 2017.

Schulz, K., Soetaert, K., Mohn, C., Korte, L., Mienis, F., Duineveld, G., and van Oevelen, D.: Linking large-scale circulation patterns to the distribution of cold water corals along the eastern Rockall Bank (northeast Atlantic), Journal of Marine Systems, 212, 103456, https://doi.org/10.1016/j.jmarsys.2020.103456, 2020.

Snelgrove, P. V. R., Soetaert, K., Solan, M., Thrush, S., Wei, C. L., Danovaro, R., Fulweiler, R. W., Kitazato, H., Ingole, B., Norkko, A., Parkes, R. J., and Volkenborn, N.: Global Carbon Cycling on a Heterogeneous Seafloor, Trends Ecol Evol, 33, https://doi.org/10.1016/j.tree.2017.11.004, 2017.

Soetaert, K., Mohn, C., Rengstorf, A., Grehan, A., and Van Oevelen, D.: Ecosystem engineering creates a direct nutritional link between 600-m deep cold-water coral mounds and surface productivity, Sci Rep, 6, 1–9, https://doi.org/10.1038/srep35057, 2016.

Thiem, Ø., Ravagnan, E., Fosså, J. H., and Berntsen, J.: Food supply mechanisms for cold-water corals along a continental shelf edge, Journal of Marine Systems, 60, 207–219, https://doi.org/10.1016/j.jmarsys.2005.12.004, 2006.

Turnewitsch, R., Dumont, M., Kiriakoulakis, K., Legg, S., Mohn, C., Peine, F., and Wolff, G.: Tidal influence on particulate organic carbon export fluxes around a tall seamount, Prog Oceanogr, 149, 189–213, https://doi.org/10.1016/j.pocean.2016.10.009, 2016.

Vic, C., Naveira Garabato, A. C., Green, J. A. M., Waterhouse, A. F., Zhao, Z., Melet, A., de Lavergne, C., Buijsman, M. C., and Stephenson, G. R.: Deep-ocean mixing driven by small-scale internal tides, Nat Commun, 10, https://doi.org/10.1038/s41467-019-10149-5, 2019.

Wang, H., lo Iacono, C., Wienberg, C., Titschack, J., and Hebbeln, D.: Cold-water coral mounds in the southern Alboran Sea (western Mediterranean Sea): Internal waves as an important driver for mound formation since the last deglaciation, Mar Geol, 412, 1–18, https://doi.org/10.1016/j.margeo.2019.02.007, 2019.

https://doi.org/10.5194/egusphere-2023-941
Preprint. Discussion started: 11 May 2023
© Author(s) 2023. CC BY 4.0 License.

Wang, H., Titschack, J., Wienberg, C., Korpanty, C., and Hebbeln, D.: The Importance of Ecological Accommodation Space and Sediment Supply for Cold-Water Coral Mound Formation, a Case Study from the Western Mediterranean Sea, Front Mar Sci, 8, 1–14, https://doi.org/10.3389/fmars.2021.760909, 2021.

Wheeler, A. J., Beyer, A., Freiwald, A., de Haas, H., Huvenne, V. A. I., Kozachenko, M., Olu-Le Roy, K., and Opderbecke, J.: Morphology and environment of cold-water coral carbonate mounds on the NW European margin, International Journal of Earth Sciences, 96, 37–56, https://doi.org/10.1007/s00531-006-0130-6, 2007.

White, M. and Dorschel, B.: The importance of the permanent thermocline to the cold water coral carbonate mound distribution in the NE Atlantic, Earth Planet Sci Lett, 296, 395–402, https://doi.org/10.1016/j.epsl.2010.05.025, 2010.

White, M., Mohn, C., De Stigter, H., and Mottram, G.: Deep-water coral development as a function of hydrodynamics and surface productivity around the submarine banks of the Rockall Trough, NE Atlantic, in: Cold-water Corals and Ecosystems, edited by: Freiwald, A. and Roberts, J. M., 503–514, 2005.

Wienberg, C., Titschack, J., Frank, N., De Pol-Holz, R., Fietzke, J., Eisele, M., Kremer, A., and Hebbeln, D.: Deglacial upslope shift of NE Atlantic intermediate waters controlled slope erosion and cold-water coral mound formation (Porcupine Seabight, Irish margin), Quat Sci Rev, 237, 106310, https://doi.org/10.1016/j.quascirev.2020.106310, 2020.

Wienberg, C., Krengel, T., Frank, N., Wang, H., Van Rooij, D., and Hebbeln, D.: Cold-water coral mounds in the western Mediterranean Sea New insights into their initiation and development since the Mid-Pleistocene in response to changes of African hydroclimate, Quat Sci Rev, 293, 107723, https://doi.org/10.1016/j.quascirev.2022.107723, 2022.

Wilson, C.: Chlorophyll anomalies along the critical latitude at 30N in the NE Pacific, Geophys Res Lett, 38, https://doi.org/10.1029/2011GL048210, 2011.